Available online www.ejaet.com

European Journal of Advances in Engineering and Technology, 2019, 6(1):84-92

Research Article ISSN: 2394 - 658X

Structural Design Optimization of A Ring Configuration Three Wing Vertical Take Off and Landing (VTOL) Scale Model using ANSYS FEA

Imran Tariq and Dr. Iqbal Rasool Memon

Department of Aeronautics and Astronautics, Institute of Space Technology, Islamabad, Pakistan -46000
imran.ist@live.com

ABSTRACT

The research work presented in this paper is carried out during the preliminary design phase of a unconventional Vertical Takeoff and Landing (VTOL) aircraft structure. Design of a scale down circular planform ring wing model has been carried out using recommended practices in the literature. A fast, stepwise and an optimized methodology is contrived which includes 3D modeling by parametric curves and automatic mesh generation abridging literature based experts recommendation. Problem setup starts with applying boundary conditions like pressure distribution and concentrated loads (engine thrust) over geometry. Finally, evaluation of structure which converges the design to an ameliorate version of geometry. The deflection and area of stress concentration are identified initially and re-analyzed after local strengthening. The iteration loop continues till the time maximum strength to weight ratio is achieved. Preliminary design (geometry version 1 or GV-1) has total weight of 3.45 kg with two wing spars, nine no of ribs and four spars in side stakes. After changes, improved structure shows satisfied deflection but weight was increased to 4.58 kg. Later, material reduction from ribs reduced its weight by 19.9% (3.63 kg), whilst increasing number of ribs to thirteen. The principle stress is reduced from 7.21 MPa to 2.34 MPa and total deflection from 6.85 to 0.547 mm at extreme loading conditions. Structural mass prediction, total directional deflection, stresses in the aircraft were key design parameters which has been calculated in this paper. The outcome of research study helps researcher, students, hobbyist etc to provide a start point of an analysis and tailored optimization methodology for structural evaluation for a series of alike unconventional aircraft geometries.

Key words: Unmanned Aerial Vehicles, Scale Models, Structural Analysis, Principle Stress & Strain, Total Deformation

1. INTRODUCTION

Scaled Balsa models are common in research which always been an area of interest for military and civil community [1]. Scale down models carry exactly similar details as the original ones. Before the invention of super computers, 3D parametric modeling and computer based design optimization it was a common practice to develop scale models to prove the concept. Arthur Sack is holding Arup S-6, a wooden scale down model aircraft shown in figure 1 (a) [2]. These scale models are build from different light weight hard and softwoods whose thickness varies as per design requirement. Strips of hard wood (Ash, Balsa, Basswood, Birch, Hickory, etc) and softwood (doughlas fir, bald cypress, Cedar and Pine) [3] ranges from 0.04 to 0.06in which may be bonded together for making desired panels [4]. Balsa is preferred as core materials in structural sandwich panels [5-6]. First Wooden monocoque structure was designed in 1911. The semi monocoque stiff structure of Vega is shown in figure 1 (b) and detail evolution of military aircraft structure can be found in Ref [7-8]. History has proven production of many small and large aircrafts built from wood and flown successfully. Many aircraft manufacturers have experienced service failure and malfunction of various devices due to insufficient rigidity, improper allowable strength, and inappropriate manufacturing tolerances. No human life onboard never recommends a lighter, fragile and unsafe structure for an aircraft or UAV [9]. A lighter structure may offer better efficiency but vulnerable to hazard in airspace as well severe threat to human life on ground. Structural fidelity analysis either from analytical approach or finite element modeling is advised prior to any design and manufacturing in order to address grey areas which are liable to encounter problems [10]. The product quality, cost and performance can be enhanced by implementing computer aided engineering analysis based on finite element methodology with effective numerical simulation and optimization [11]–[13].

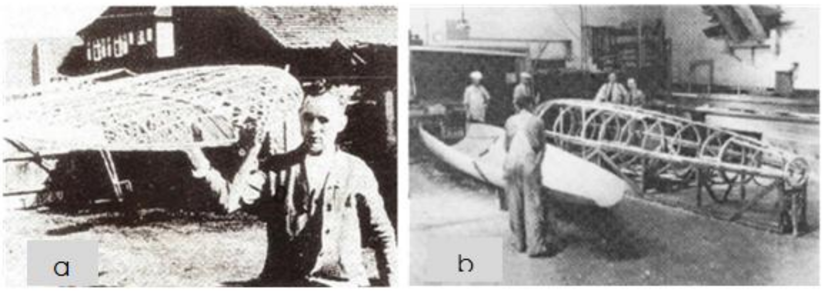

Fig .1 (a) Arthur Sack holding scale down of AS-6 **(b)** Semi-monocoque wooden fuselage

An easy and simple approach is developed to carry out preliminary structural analysis study. The main goal is to achieve better results by the use of minimum computational. The degree of freedom and nodes will require larger computational facility, time and increased cost. To get better distribution of loads certain manufacturing constrains are to be removed [14].

PRELIMINARY GEOMETRY DESIGN

Our model is a uniquely configured low subsonic UAV which has capability to takeoff / land vertically through a single engine ducted propeller. It is a three wing annular (circular) planform aircraft. Three wings are categorized as the main wing, side stakes, and horizontal stabilizer as shown in figure 3 (a). It will be carrying 500 grams of payload (HD camera) for reconnaissance purpose at a 37m/s with cruise altitude of 3000m. The main wing has distributed span wise airfoil sections (ribs), spars to support the wing bending, skin to bear pressure and control surfaces. Main wing has a span of 1.31m and root chord of 0.67m. The structural model is designed as per recommendations in the literature [15]–[17]. Standard structural supporting members like ribs, spars, bulkhead, stringers and skin is used. The leading edge (fore) spar is located at 33% and trailing edge (aft) spar is 73.5% of chord initially. It has flaperons in the main wing. However, for analysis simplification all the control surfaces have been removed. The E591 airfoil is selected for main wing (pointed out by leader no 2 in figure 3 has a maximum thickness of 16.92% at 26.3% of chord. Balsa skin (2mm thick) covers the whole frame. The leading edge radius is 3.107%. The fuselage will be carrying electronics bay and a fuel tank for the engine which is supported by bulkheads. The horizontal tail is a simple flat plate. The leader 2 shows the side stake. It starts from Rib no 7 to Rib No 10 and have NACA 0012 a symmetric airfoil with 12% thickness at 30% of chord with leading edge radius of 1.493%. Two vertical fins pointed out by leader 5 is carrying NACA 0012 (figure 3) with root chord of 0.22m. Summary of the aircraft geometry parameters are listed in table 1.

Table -1 Summary of Aircraft Geometry

Parameter	Value	Parameter	Value
Sref	1.21 m^2 / 12.99ft^2	Root Chord Stakes	1.3m / 4.26ft
Main Wing Span	1.31m / 4.287ft	Tip Chord Stakes	0.14m/ 0.47ft
Root Chord Main Wing	0.67m / 2.2ft	Aspect Ratio	2.68
Tip Chord Main Wing	0.39m / 1.28 ft	Total Length	2.1m / 6.88ft
Side Stakes Span	0.262m / 0.86 ft	Circular Disk Diameter	1.83m / 6 ft

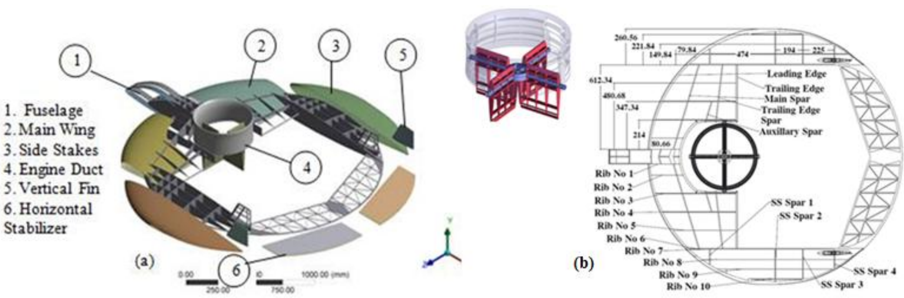

Fig. 2 (a) Aircraft Exploded View **(b)** General dimensions (right)

Material mainly used in the model is BALSA and its properties are given in the table below

Table -2 Structural Detail of Geometry

Profile	Thick. (mm)	Material	Grain Axis Direction	Description
Rib No 1,3,7,8,10	2	Ply	Along X	Additional load carrying ribs
Rib No 2,4,5,6,9	1.67	Balsa	Along X	Normal ribs to maintain profile
SS Spar 1,2,3,4	6	Ply	Along Y	To support the side stakes
Leading Edge	6/8	Ply/Balsa	Along Y	Strips of ply and balsa are glued together
Trailing Edge	2/6/2	Ply/Balsa/Ply	Along Y	
Leading Edge Spar	2/6/2	Ply/Balsa/Ply	Along Y	
Auxiliary Spar	6	Balsa	Along Y	Supports the rib bearing duct load
Trailing Edge Spar	4	Balsa	Along Y	Located at 73.5% of chord
Horizontal Tail	3.5	Balsa	Along Y	Flat Plate with truss
Vertical Tail		Balsa	Along Z	Airfoils/Spars made of Balsa
Duct Rib / Vanes	2	Balsa	Along Z/Y	All made up of balsa

METHODOLOGY

Professional modeling and analysis utilizes global / local approach in which localized components like ribs, spars etc of an aircraft are baseline stress optimized and further utilized in assemblies. It saves material, computation cost and produces better optimized solution after several bottom / top iterations [18]. Many researchers have used commercially available packages to evaluate the structural model of UAV [19]. To carry out the static structural analysis of the wing and determination of stress distribution on the wing ANSYS is commonly used [20]. The entire process starts with importing the geometry to the pre-processor solver [21]. An easy and simple approach is developed here to carry out preliminary structural analysis. The main goal is to optimized structure having minimum weight and maximum strength, by the use of minimum computational power with certain assumptions. Each iteration will enhance the bearing load as compared to previous version. As degree of freedom is dependent on number of components attached in an assembly and larger number of component will require larger computational facility, time and increased cost [22]. To get better distribution of loads certain manufacturing constrains are removed [14]. A concoction of different techniques including 3D parametric modeling, suitable mesh generation of the model, FEA study to find out planar deformations with localized stresses using commercially available package (ANSYS).

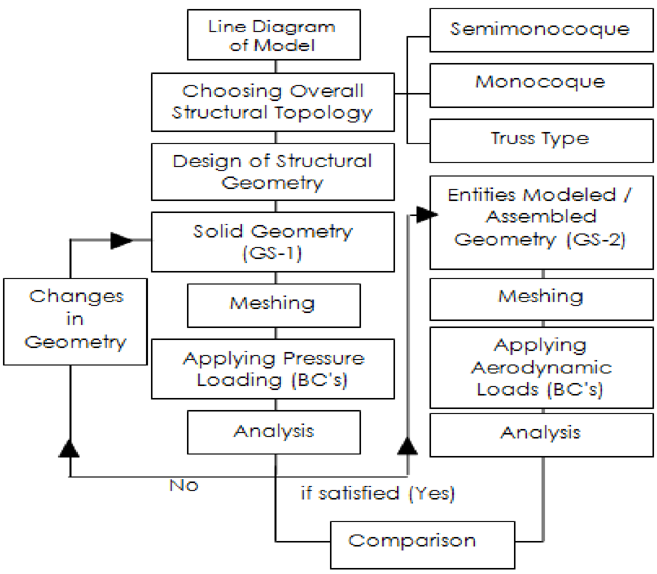

Fig. 3 Methodology for Analysis

Lift distribution on the wing has been calculated by aerodynamics group which is applied on structure by simply creating a link between results from CFD to Structural module. The pressure loading is transferred to analysis setup automatically. Point load application at designated places are identified and known load is applied at the ducted fan engine bracket which was available from literature. Later, calculation of static strength and deflection of the model is carried out. All the possible and maximum loads an aircraft can experience is simulated with a safety factor of 1.5 [23]. The structural geometry version 1 (GV-1) is a starting reference. To save computational cost and power initial calculations and iterations are carried out on GV-l. Later the changes are made in this geometry to release a second version GV-2. The meshing metrics are noted down and boundary condition is applied. After the analysis key parameters like weight with stress distribution and concentration has been recorded and repeated it till satisfactory results are obtained and a final model is generated. A stepwise and easy methodology (as shown in figure 3) is worked out in this research work which can be used as a reference to carry out preliminary optimization of structural design for any model aircraft having unconventional geometry

BOUNDARY CONDITION / PROBLEM SETUP

Assumptions

Internal components such as fuel tank, electronics, and cables are disregarded and not incorporated for structural analysis. Material is perfect, no crack / flaw exists in the whole structure. The structural components are perfectly bonded together with perfectly defined mesh connections and assumed to transfer load as taken by individual component. Stiffness of the material is linearly dependent on the density (solid isotropic material with penalization). The material density is directly used as design variable. All analysis was conducted considering only the structural support provided by spars, ribs, and internal structure of the wing. The skin of the UAV is removed in analysis and as it will add to the safety factor.

Loading

Aerodynamic loads can be found theoretically [24] as well as numerically in many different ways. Prandtl lifting line theory, Swept wing theory, Low Aspect Ratio Wing Theory or spectral methods etc are being used widely for theoretical evaluation. Some tools like tornado, Xfoil or digital DATCOM can also be used to find out aerodynamic loading. DATCOM cannot deal with complex geometries like circular configurations. In our case the aerodynamic loading was available from the CFD analysis which was carried out using FLUENT. The pressure distribution for different angle of attack is shown in figure 4. The aerodynamic loading was directly taken onto the structural model by ANSYS loading interface. Also concentrated load like thrust on the duct was applied which is available in literature and Blanchete has measured it experimentally [25].

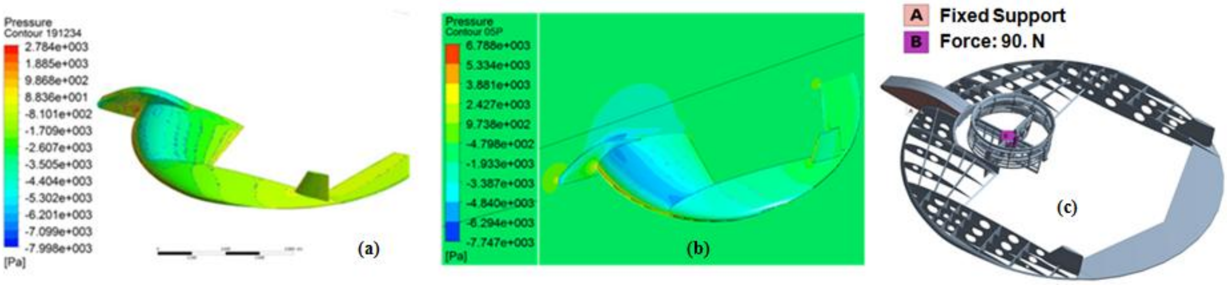

Fig. 4 Pressure distribution (a) zero degree angle of attack (AOA) (b) 14 deg AOA (c) Applied Concentrated Loads

Material

Material selection is an important task designer has to undertake during its design. Wood is porous anisotropic material exhibiting different properties in axial, lateral and transverse directions. Density values for balsa typically range between 100 and 360, for ply it ranges from 300-800 kg/m3. Mechanical performance of balsa is strongly dependent on its density. The axial compressive strength, shear modulus and Young's modulus increase linearly with increase in density [6, 26-27]. Transverse compressive modulus and strength values are about an order of magnitude lower than those in the axial direction. The transverse compressive modulus and strength are higher in the radial than in the tangential direction because the rays act as reinforcement. For most practical purposes balsa wood is taken as transversely isotropic with anisotropic plane perpendicular to axis of tree. The structure of wood as shown in figure 5 as longitudinal (L), radial (R) and tangential (T) planes of elastic symmetry. Balsa Wood, Ply wood and carbon fiber with epoxy resin is selected for our UAV structure.

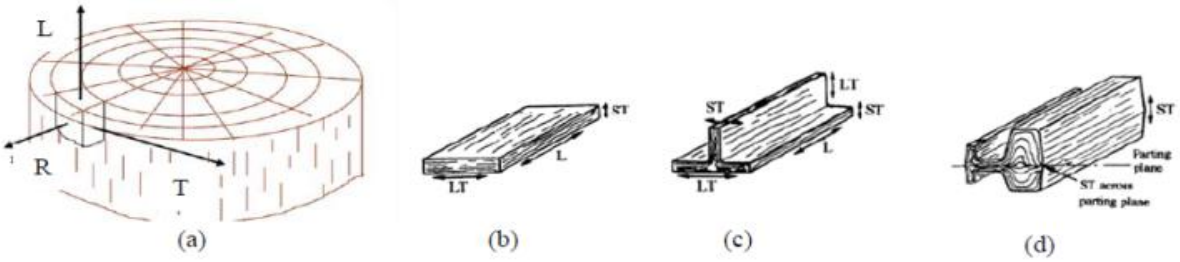

Fig. 5 Principle Direction in Wood, Plate and Strip/Sheet

Table- 3 Material Properties

Property	Sym	Unit	Balsa	Ply [28]
Parallel Normal Modulus	EL	GPa	5.30	-
Perpendicular Normal Modulus	ET	GPa	0.20	-
Parallel Shear Modulus	GLT	GPa	0.166	0.138-0.207
Perpendicular Shear Modulus	GLR	GPa	0.085	0.586-0.758
Parallel Tensile Strength	LT	GPa	0.0135	27.6-34.5
Perpendicular Tensile Strength	ST	GPa	0.0004	-
Parallel Shear Strength	SLT	GPa	0.003	1.72-2.07
Parallel compressive Strength	LC	GPa	0.0127	31-41.4
Perpendicular compressive Strength	SC	GPa	0.0023	-
Perpendicular Shear Strength	SST	GPa	0.004	5.52-6.89
Density	rho	kg/m^3	155	500-650

Mesh

Most of the engineering geometries are discretized using tri/tetra or quadrilateral mesh elements. Quadrilateral mesh has better quality and convergence. It is implemented by direct or indirect approach. Generally, direct approach is more difficult to handle [29], but on the other hand tetrahedral mesh generation always satisfies the close boundaries, line constrains or complex geometries in automatic mesh generation [30]. The algorithm behind it always carry out optimization of the mesh skewness. The manual face paving or mapped mesh always confronts difficulty or bad mesh element at the complete curves which is time consuming process more prone to error generation. However, post processing the mesh can improve efficiency and smooth it [31]. Keeping in view the major classification criteria for mesh which includes geometry factor, mesh type, element type, density and time automatic triangular mesh with iteratively automatic smoothing has been selected for the application on this geometry. Since, good mesh generation is an important aspect to produce good results (<10 %error), Hollister found out that minimum 2-4 elements are required across the thickness of digital mesh [32]. Due to limitation of computational resources one cannot always meet the minimal mesh density in all parts and geometrically complex mesh may not be appropriate [33]. Figure 6 shows few selected views from all the versions of geometry. GV-1 has 1.245 million elements having minimum element size of 0.004m. However, the max element size was kept at 2mm. The local minimum was 0.0007mm to accommodate the sharp edges in the duct. The element quality is satisfactory because it matches the recommended skewness and orthogonality values. Initially, many numbers of elements like 0.2 M, 0.5M , 0.7M were tried on the two geometries but that didn't showed consistency in the results and improving geometry didn't improve the total deformation or stresses. Table 4 reports the summary of the generated mesh along with time taken for all three geometries.

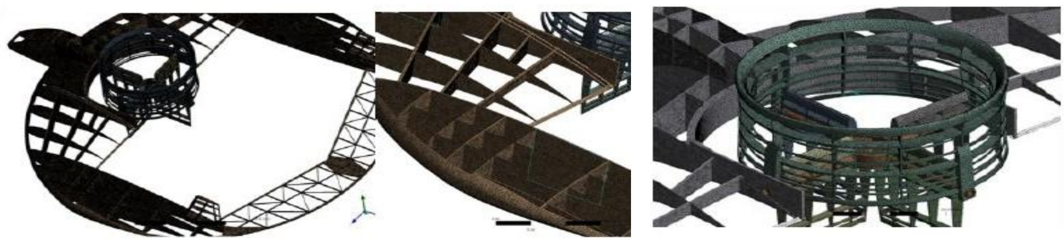

Fig. 6 Glimpse of Mesh generated for Analysis

Table -4 Mesh metrics

Geometry Vwesions	Size Func./Type/ Elements (M) / Level	Time Cons(min)	Min. Elem Size (mm)	Average Quality	
				Orthogonality	Skewness
GV-1	Fixed/Tetra/1.245M/Fine	42	0.004	0.80	0.463
GV-2	Fixed/Tetra/1.159M/Fine	45	0.004	0.81	0.451
GV-3	Fixed/Tetra/1.556M/Fine	54	0.0037	0.86	0.474

PRELIMINARY ANALYSIS

Preliminary analysis is carried upon geometry version 1 (GV-1) and total deformation, principle stress and shear stresses are calculated by applying aerodynamic load, fixed support at fuselage, and thrust concentrated load of 90.0 N. The significance of basic analysis is that it provides a good starting point for estimation of weight, strength of structure and later the designer could generate an improved versions of geometry. The solution was obtained in approximately 43 minutes with maximum deformation of 6.85 mm at tail section. The deformation value is not acceptable as structure may break from spar no 2. Tail has maximum deflection which decreases gradually to 3.45mm in side stakes and 0.21mm in main wing. The principle stress comes out to be max 7.2 MPa at the trailing edges of an airfoil. The ribs thickness distribution in the main wing is satisfactory except for the region holding the duct, but the spars are not enough to hold the side stakes and side stakes are not strong enough to hold the horizontal stabilizer. Figure 7 (a) shows the total deformation and figure 7 (b) is illustrating the total principle stress.

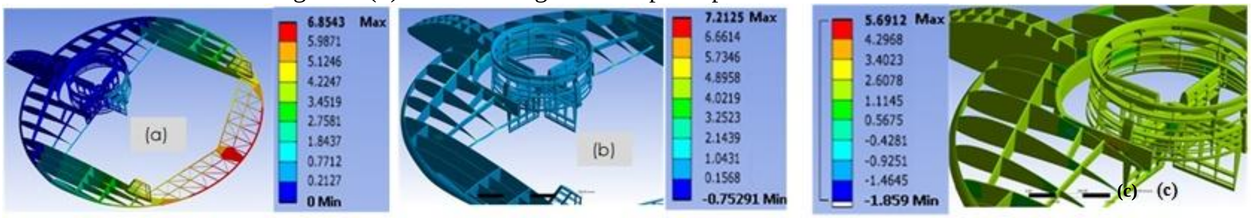

Fig. 7 (a) Total Deformation (mm), **(b)** Max. Principle Stress (MPa), **(c)** Max. Shear Stress (MPa)

The principle stress is concentrated at the interface between the wing and duct attachment. The local stress concentration revealed that this part has to be strengthen more to hold the downward thrust. All the stress concentration problems are addressed changing the structural elements and incorporated in design to generate the version 2 of the geometry. Negative stress shows that the rib is squeezing as wing bends. A large shear was expected along the span but maximum value of shear is pointed out 5.69 MPa (figure 7c) which is due to thrust loading. Overall average shear value in the whole structure is high (2.6MPa) and it could only be reduced by strengthening the geometry.

RESULTS & DISCUSSION

Design Modification

Structural improvements are made after analyzing the GV-1. The key modification includes increasing number of ribs from 10 to 13 in the main wing to rigidly support duct and side stakes. The thickness of the horizontal tail is also improved from 3.5mm to 5mm. Adding spars to the side stakes and its number increased from 4 to 7 which will support the tail as well. Reiterating main wing spar distribution is also made and total number of spars in the main wing has been increases to 3. Three main spars are running throughout the wing section. The leading edge spar is re-located at 18 % of chord, center wing spar is at 48.6%, auxiliary and trailing edge spar location remains unchanged. Figure below shows the dimensions after making necessary changes.

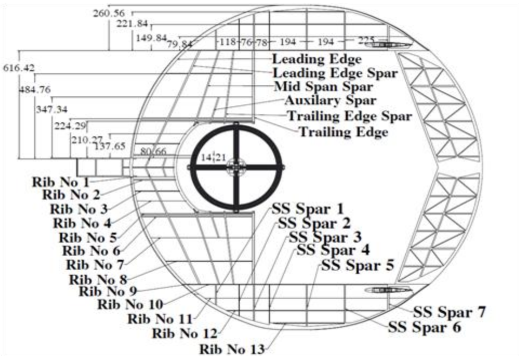

Fig. 8 Geometry V2, Sketch after changes

It is expected that the deflection in the tail will be reduced with overall reduction in shear and normal stress after improving the geometry. Figure 8 shows an updated version of geometry and Table 5 contains the modification made in the earlier version of geometry (as listed in table 2). The re-analysis revealed that, changes made in horizontal tail thickness and an addition of side stake spars reduces deflection significantly.

Table -5 Geometric changes of Version 2

Profile	**Geometry 2**	
	t (mm)	**Material**
Rib No 1,3,4,9,10	2	Ply
SS Spar 1,2,3,4,4,5,6,7	6	Ply
Leading Edge Spar	2/6/2	Ply/Balsa/Ply
Auxiliary Spar	6	Balsa
Rib No 2,5,6,7,8,11,12,13	1.67	Balsa
Horizontal Tail	5	Balsa
Main Spar	2/6	Ply Balsa
Trailing Edge Spar	4	Balsa

Figure 9 shows the total deformation in the structure, principal stress distribution and maximum shear stress distribution respectively. Now, deflection comes out to be 3.75mm in the horizontal tail section, but still geometry requires improvement. In the 3rd version of geometry horizontal tail thickness is further increased from 5mm to 6mm, thickness of spar lying at the center (8mm to 18mm) and Rib no 10 (from 2 to 4mm (ply)). The trailing edge thickness was also changed from 10mm to 25mm All the sharp corners were stiffened by introducing small triangular supports. The detail of changes made is shown in figure 10.

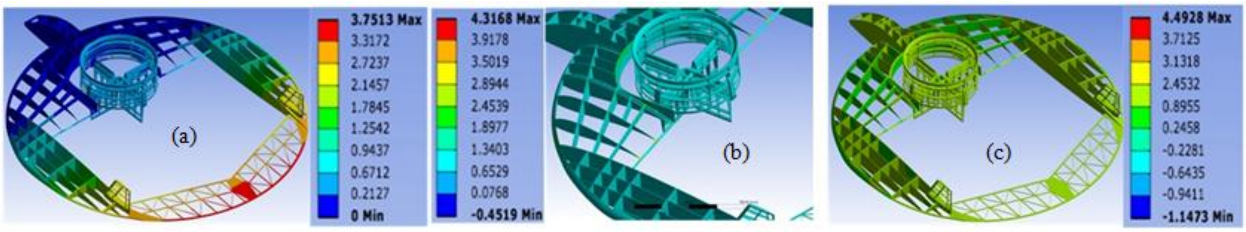

Fig. 9 (a) Total Deformation (mm), **(b)** Max. Principle Stress (MPa), **(c)** Max. Shear Stress (MPa)

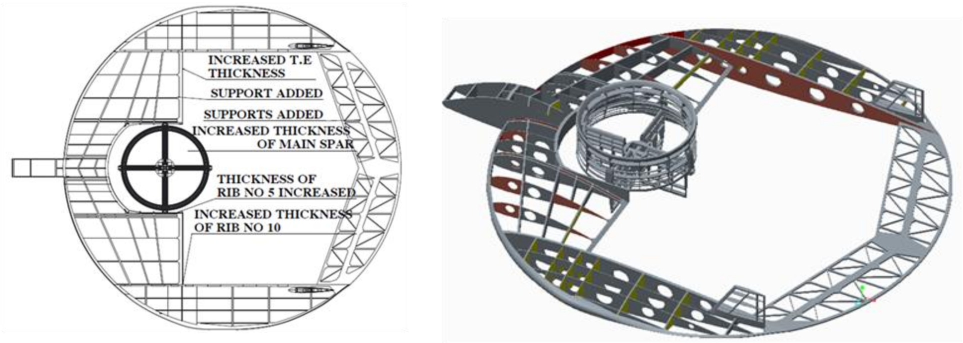

Fig. 10 After changes in geometry V2

The only problem faced during final iteration was increase in the weight. The aero group has constrained the weight to 3.7kg. The conventional weight reduction technique is employed to reduce the weight and introducing the holes in the ribs has reduced the total weight by 19.9% (3.67kg) in comparison to previous geometry. Also, the stress concentration at severely loaded members or total deflection lies within acceptable range. The tail deflection which was a major issue in the previous versions of geometry is 0.54mm only. The tensile strength in the grain direction is 13.5 MPa.

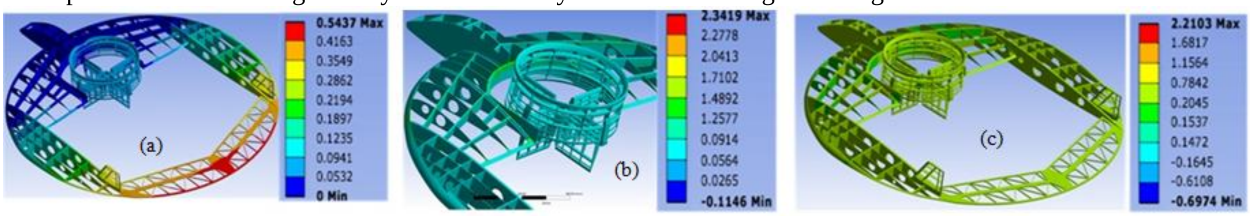

Fig. 11 (a) Total Deformation (mm), **(b)** Max. Principle Stress (MPa), **(c)** Max. Shear Stress (MPa)

The figure 11 shows that final value of principal stress is 2.341 MPa and it will not yield at the time of actual loading. Table No 6 shows comparison of results summarized before and after the optimization of structure.

Table -6 Summary of Analysis

Properties		**G V1**	**G V2**	**G V3**
No of Ribs		10	13	13
No of Spars		2	3	3
Side Stake Spars		4	7	7
Total Weight (kg)		3.45	4.58	3.67
Maximum	Principal Stress (MPa)	7.2125	4.3168	2.3419
	Shear Stress (MPa)	5.6912	4.4928	2.2103
	Deflection (mm)	6.8543 4	3.7513	0.5437 0
Time Consumed (min)	Mesh	42	45	54
	Analysis	85	77	91

CONCLUSION

The research work leads to a conclusion that for a quick structural analysis at preliminary design stage researcher, student or hobbyist can make two/three spar wing model. Two spar can be distributed in a way that leading edge (L.E) spar may lie in between 16-27% and trailing edge spar 50-70% respectively. Placement of trailing edge (T.E) spar also depends upon considerable thickness of airfoil. Three spar wing will have L.E spar between 5-18 %, Middle spar in the mid chord and T.E spar between 65-80%. Ribs structure distribution is intuitive such that it could compensate the shearing effect of wind load. A 1.5-3mm of balsa strip is recommended for skin on wing for aircraft ranging from trainer to aerobatic aircraft. A maximum three number of iterations will reveal a design of choice for the scale down model aircrafts with the design methodology established and presented in the paper.

REFERENCES

[1]. M. Hassanalian, and A. Abdelkefi, "Classifications, applications, and design challenges of drones: A review," *Progress in Aerospace Sciences*, 2017, vol. 91, pp. 99–131,.

[2]. David Myhra, PhD, *Sack AS 6- Source of Nazi Germany UFO Claims?* RCW Technology & Ebook Publishing, 2013.

[3]. F. P. Laboratory (U.S.), *Design of Wood Aircraft Structures*, Subcommittee on Air Force-Navy-Civil Aircraft Design Criteria, Munitions Board, Aircraft Committee, 1951.

[4]. M. Loughead, "Process of manufacturing curved forms of plywood or fibrous compositions," US1425113 A, 1922.

[5]. Andre Da Silva and Stelios Kyriakides, "Compressive response and failure of balsa wood," *International Journal of Solids and Structures*, 2007, vol. 44, no. 25–26, pp. 8685–8717,.

[6]. Marc Borrega and Lorna J.Gibson, "Shear mechanical characterization of balsa wood as core material of composite sandwich panels," *Constr. Build. Mater.*, 2013, vol. 41, pp. 231–238,.

[7]. D. Paul, T. Hess, and E. Kautz, "The evolution of U.S. military aircraft structures technology," in *American Institute of Aeronautics and Astronautics 37th Structure, Structural Dynamics and Materials Conference*,. Salt Lake City, U.S.A. 1996

[8]. D. Paul, L. Kelly, V. Venkayya, and T. Hess, "Evolution of U.S. Military Aircraft Structures Technology," *Journal of Aircraft*, 2002, vol. 39, no. 1, pp. 18–29,.

[9]. A. Majka, Flight Loads of Mini UAV, *Solid State Phenomena* vol. 2013, 198:194-199 ·

[10]. Wahyu Kuntjoro, "An Introduction to the Finite Element Method,". Web. https://www.bookdepository.com/Introduction-Finite-Element-Method-Wahyu-Kuntjoro/9780071241441, May 2006

[11]. Joseph P. Elm and John E. Robert, "Integration of Computer-Aided Design and Finite Element Analysis Tools in a Small Manufacturing Enterprise." *Technology Insertion, Demonstration, and Evaluation Program*, 2003.

[12]. Z. Q. Guan et al., A finite element parametric modeling technique of aircraft wing structures, *Chinese Journal of Aeronautics*, 2013, Volume 26, Issue 5,

[13]. J. Austin, Thomas J. R. Hughes, and Yuri Bazilevs, "Isogeometric Analysis: Toward Integration of CAD and FEA," Wiley.com. Web. https://www.wiley.com/en-us/Isogeometric+Analysis%3A+Toward+Integration+of+CAD +and+FEA-p-9780470748732, Sep 2009

[14]. D. Walker and D. Liu, "Topology Optimization of an Aircraft Wing," in *American Institute of Aeronautics and Astronautics 56th AIAA/ASCE/AHS/ASC Structures, Structural Dynamics, and Materials Conference*, Kissimmee , Florida, 2015, AIAA 2015-0976

[15]. M. C. Y. Niu, Composite airframe structures: practical design information and data. Conmilit Press, 1992.

[16]. Mark D. Sensmeier and Jamshid A. Samareh, "A Study of Vehicle Structural Layouts in Post-WWII Aircraft." *45th AIAA/ASME/ASCE/AHS/ASC Structures, Structural Dynamics and Structures Conference; 19-23;* Palm Springs, CA; United States, Apr 2004

[17]. C. Niu and M. C.-Y. Niu, Airframe Structural Design: *Practical Design Information and Data on Aircraft Structures*. Adaso Adastra Engineering Center, 1999.

[18]. L. Krog, A. Tucker, G. Rollema, and A. Uk Ltd, Application of topology, sizing and shape optimization methods to optimal design of aircraft components, *Altair Engineering*, web. https://pdfs.semanticscholar.org/01bf/fdc70353edca8813166bc3eb9d58285ed629.pdf, 2018.

[19]. Prof. Dr. Muhsin J. Jweeg, Dr. Shawkat J. AL-Tornachi, and Salah H. Abid-Aun, "Optimization of Light Weight Aircraft Wing Structure," Journal of Engineering Development, vol. Vol. 12, No. 1, March 2008.

[20]. Sercan Soysal, "*Structural Design, Analysis And Composite Manufacturing Applications For A Tactical Unmanned Air Vehicle*." Middle East Technical University, Turkey, May 2008.

[21]. Juha Kortelainen, "Meshing Tools for Open Source CFD – A Practical Point of View.", VTT-R-02440-09, https://www.vtt.fi/inf/julkaisut/muut/2009/VTT-R-02440-09.pdf, *CSC – IT Center for Science Ltd*, Finland, Apr 2009.

[22]. Y. Liu, "*Efficient* Methods for Structural Analysis of Built-Up Wings," *Virginia Polytechnic Institute and State University*, Apr 2000.

[23]. F. Gern, "Finite Element Based HWB Center body Structural Optimization and Weight Prediction," *31st Aerodynamic Measurement Technology and Ground Testing Conference*; Dallas, AIAA, TX; United States, 2015.

[24]. R. J. Margason and J. E. Lamar, "Vortex-lattice FORTRAN program for estimating subsonic aerodynamic characteristics of complex planforms," web. https://ntrs.nasa.gov/search.jsp?R=19720000617, Oct 1972.

[25]. Bryan M. Blanchette, "*Vehicle The Design And Construction Of A Ship Launched VTOL Unmanned Air Vehicle*," Thesis, Naval Postgraduate School, 1990.

[26]. M. Vural and G. Ravichandran, "Dynamic response and energy dissipation characteristics of balsa wood: experiment and analysis," *International Journal of Solids Structures*., 2003, vol. 40, no. 9, pp. 2147–2170.

[27]. G Newaz, M Mayeed, and A Rasul, "Characterization of balsa wood mechanical properties required for continuum damage mechanics analysis." Proceedings of the Institution of Mechanical Engineers, *Journal of Material: Design and Applications*. 2016, Vol. 230(1) 206–218.

[28]. Bal, B. C., & Bektaþ, Ý "Some mechanical properties of plywood produced from eucalyptus, beech, and poplar veneer,". *Maderas. Ciencia y Tecnología*, 2014, 16(1); 99-108.

[29]. Chae S W and Jeong JH, "Unstructured surface meshing using operators." *Proceedings of the Sixth International Mesh Round Table*, Park City, Utah, 1997.

[30]. Kyu-Yeul Lee, In Il Kim, Doo-Yeoun Cho, and Tae-wan Kim, "An algorithm for automatic 2D quadrilateral mesh generation with line constraints -." *Computer Aided Design*, *Science Direct*, 2003 pp. 1055–1068.

[31]. K. Ho-Le, "Finite element mesh generation methods: a review and classification," *Computer Aided Design*, 1988, vol. 20, no. 1, pp. 27–38.

[32]. R. T. Hart, V. V. Hennebel, N. Thongpreda, W. C. Van Buskirk, and R. C. Anderson, "Modeling the biomechanics of the mandible: A three-dimensional finite element study," *Journal of Biomechanics*, 1992, vol. 25, no. 3, pp. 261–286.

[33]. D. L. A. Camacho, R. H. Hopper, G. M. Lin, and B. S. Myers, "An improved method for finite element mesh generation of geometrically complex structures with application to the skull base," *Journal of Biomechanics*, 1997, vol. 30, no. 10, pp. 1067–1070.